

Enhanced Quantum Synchronization via Quantum Machine Learning

F. A. Cárdenas-López,^{1,2,*} M. Sanz,^{3,†} J. C. Retamal,^{1,2} and E. Solano^{3,4}

¹*Departamento de Física, Universidad de Santiago de Chile (USACH), Avenida Ecuador 3493, 9170124, Santiago, Chile*

²*Center for the Development of Nanoscience and Nanotechnology 9170124, Estación Central, Santiago, Chile*

³*Department of Physical Chemistry, University of the Basque Country UPV/EHU, Apartado 644, 48080 Bilbao, Spain*

⁴*IKERBASQUE, Basque Foundation for Science, Maria Díaz de Haro 3, 48013 Bilbao, Spain*

We study the quantum synchronization between a pair of two-level systems inside two coupled cavities. Using a digital-analog decomposition of the master equation that rules the system dynamics, we show that this approach leads to quantum synchronization between both two-level systems. Moreover, we can identify in this digital-analog block decomposition the fundamental elements of a quantum machine learning protocol, in which the agent and the environment (learning units) interact through a mediating system, namely, the register. If we can additionally equip this algorithm with a classical feedback mechanism, which consists of projective measurements in the register, reinitialization of the register state and local conditional operations on the agent and register subspace, a powerful and flexible quantum machine learning protocol emerges. Indeed, numerical simulations show that this protocol enhances the synchronization process, even when every subsystem experience different loss/decoherence mechanisms, and give us flexibility to choose the synchronization state. Finally, we propose an implementation based on current technologies in superconducting circuits.

PACS numbers: Machine Learning, Quantum Information processing, Quantum Synchronization.

INTRODUCTION

Artificial intelligence (AI) and machine learning (ML) have attracted much attention in the last decade. ML consists of computational algorithms which can improve their performance, even though this improvement has not been explicitly programmed [1]. Several fields such as economy [2], medicine [3, 4], pattern recognition systems [5, 6], or social media [7] profited from the advantages offered by ML. Essentially, there are three types of learning in ML, namely, supervised learning, unsupervised learning and reinforcement learning [8]. In supervised learning the system learns from initial data to make future decisions. Regression (continuous output) and classification (discrete output) are considered as archetypical supervised learning algorithm. In unsupervised learning, the classes are not defined from the beginning (classification), but they naturally emerge from the initial data. In other words, the data is organized in subsets based on correlations found by the algorithm. Data clustering is the most usual example of unsupervised learning algorithm. In reinforcement learning [9] there is a scalar parameter, named rewarding, which evaluates the performance of the learning process. Depending on the rewarding, the system can decide whether the learning process is optimized or not. Recently, a novel perspective of using ML algorithms to enhance quantum tasks has emerge, particularly by using genetic algorithms [10, 11].

Synchronization phenomena refers to a set of two or more self-sustained oscillators with different frequencies that are forced to oscillate with a common effective frequency [12, 13]. The interaction between systems modifies the frequency at which each system oscillates. This phenomenon has been observed and used in biological systems [14, 15], engineering [16], geolocalization, just to name a few. During the last decade, a significant progress has been made in the development of quantum platform such as trapped ions [17, 18],

nanomechanical resonator [19–21] as well as superconducting circuit and circuit quantum electrodynamics (cQED) [22–24]. This important progress has made possible to study the synchronization phenomena at the quantum level [25–31]. Initially, arrays of quantum harmonics oscillators were studied. These systems show the advantages that they have a classical limit, since they can be effectively treated as classical systems when the oscillators have many excitations. This allows a natural comparison between classical and quantum synchronization. However, the study of synchronization in quantum systems without a classical counterpart such as two-level systems becomes non-trivial and controversial. It has to be studied, among other techniques, through the natural observables of these systems [32–34].

In this article, we address how synchronization phenomena can be understood as a machine learning protocol. Our proposal relies on the digitization of the master equation that governs the system dynamics. We show that the digitized dynamics leads to the same result obtained in the analog case. Furthermore, we can identify all the fundamental elements of a quantum machine learning protocol. In this sense, we find that the synchronization of the two qubits can be enhanced when we add a feedback mechanism to machine learning protocol. Finally, we propose an implementation with current technology in superconducting qubits.

DIGITIZED QUANTUM SYNCHRONIZATION

Let us consider a system composed by two dissipative cavities containing each one a two-level system. Both cavities interact via hopping interaction, and a coherent driving field acts in one of the two-level system to counterbalance the dissipation present in both cavities. The dynamics of the system

is described by the master equation ($\hbar = 1$).

$$\dot{\rho}(t) = -i[\mathcal{H}, \rho] + \kappa \sum_{\ell=1}^{N=2} (2a_{\ell}\rho a_{\ell}^{\dagger} - a_{\ell}^{\dagger}a_{\ell}\rho - \rho a_{\ell}^{\dagger}a_{\ell}), \quad (1)$$

where the Hamiltonian \mathcal{H} is expressed in the rotating frame with respect to the laser field as

$$\begin{aligned} \mathcal{H} = & \sum_{\ell=1}^{N=2} \left(\Delta_{\ell} a_{\ell}^{\dagger} a_{\ell} + \frac{\delta_{\ell}}{2} \sigma_{\ell}^z + ig(-1)^{\ell} (a_{\ell}^{\dagger} \sigma_{\ell}^{-} - a_{\ell} \sigma_{\ell}^{+}) \right) \\ & + \Omega \sigma_1^x - J(a_1^{\dagger} a_2 + a_1 a_2^{\dagger}). \end{aligned} \quad (2)$$

Here, $a_{\ell}^{\dagger}(a_{\ell})$ is the creation (annihilator) boson operator of the ℓ th field mode, while σ_{ℓ}^k stands for the k -component Pauli matrix. $\Delta_{\ell} = \omega_{p,\ell} - \omega_d$ is the detuning between the ℓ th field mode $\omega_{p,\ell}$ and the driving frequency ω_d , also $\delta_{\ell} = \omega_{q,\ell} - \omega_d$ stands for the detuning between the ℓ th qubit frequency $\omega_{q,\ell}$ and the driving frequency, and g is the coupling strength between the field mode and the two-level system. Finally Ω corresponds to the strength of the driving field, J is the coupling strength between cavities, and κ is the decay rate for the cavities. In this system configuration, it is already proven that quantum synchronization between observables of two qubits is achieved [35].

Our approach to this problem is to analyze the quantum synchronization of the two qubits by considering a digital-analog version of the master equation given in Eq. (1). We show that both digital-analog simulation yield the quantum synchronization. The decomposition of the master equation into digital steps is shown in Fig 1. We can discriminate two different types of interactions in this decomposition, namely, non-local gates or analog block and local gates or digital terms. Analog blocks are associated with the interaction terms in Hamiltonian in Eq. (2), which correspond to Jaynes-Cummings and hopping terms. The dynamics associated with these terms can be implemented by the unitary operations $U_{q_{\ell}, p_{\ell}}$ ($\ell = 1, 2$) and U_{p_1, p_2} defined as

$$U_{q_{\ell}, p_{\ell}} = e^{-ig(-1)^{\ell} (a_{\ell}^{\dagger} \sigma_{\ell}^{-} - a_{\ell} \sigma_{\ell}^{+}) \Delta t} \quad (3a)$$

$$U_{p_1, p_2} = e^{iJ(a_1^{\dagger} a_2 + a_1 a_2^{\dagger}) \Delta t} \quad (3b)$$

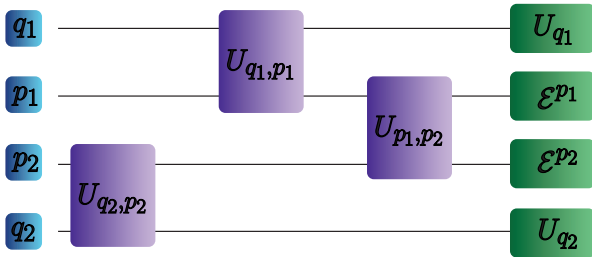


FIG. 1: Schematic diagram for the digitized system dynamics. The purple block represent the global gates, while the green ones correspond to the local gates.

On the other hand, local gates are associated with the unitary dynamics of the free Hamiltonian in Eq. (2), and the dissipative dynamics of the Lindbladian terms of the master equation in Eq. (1). For both qubits, the local gates only correspond to the evolution of their respective free Hamiltonians,

$$U_{q_1} = e^{-i(\delta_1 \sigma_1^z / 2 + \Omega \sigma_1^x) \Delta t}, \quad (4a)$$

$$U_{q_2} = e^{-i\delta_2 \sigma_2^z \Delta t / 2}. \quad (4b)$$

For cavities, the local operations are represented by the dynamical map given by the master equation

$$\dot{\rho}(t) = -i[\Delta_{\ell} a_{\ell}^{\dagger} a_{\ell}, \rho] + \kappa(2a_{\ell}\rho a_{\ell}^{\dagger} - a_{\ell}^{\dagger}a_{\ell}\rho), \quad (5)$$

for a time Δt . Now we want to compute the expectation values of the observables of both two-level system (q_1 and q_2) using the digitized master equation and compare them with the expectation values obtained by directly solving the master equation Eq. (1). In Fig 2, shows the numerical simulations for the expectation values of Pauli matrices $\{\sigma^x, \sigma^y, \sigma^z\}$ for the qubit q_1 obtained by both methods. The calculation is carried out for a sufficiently large number of steps (κt divided into 100 parts). As we infer from these results both approaches are equivalent.

We will show that if we interpret the proposed digitized terms of the master equation as a machine learning protocol in which qubits learn from each other, we would improve the speed of this learning procedure. Indeed, in a recent proposal for reinforcement quantum learning [10, 36], the agent and the environment do not directly interact, and the learning process is mediated by an ancillary system, namely the register. In our setup, the synchronization between both qubits is similarly carried out through the field modes. In this case, we can identify the agent and the environment with the qubit q_1 and q_2 , respectively, while the register is identified with the field modes. With the novelty that the register is now connected to a decoherence channel. In our case, the interactions among the elements are given by the digital-analog blocks. Therefore, under this identifications, the digitized master equation can be considered as a machine learning protocol, but without a feedback mechanism. In the following section, we will introduce the feedback mechanism in order to improve the learning protocol.

ENHANCED QUANTUM SYNCHRONIZATION

In this section, we will study a more general situation of three two-level systems, each of them identified with a learning units; agent, environment and register. Notice that the previous case is equivalent to this one, since we study a case in which we are far below one excitation in the system, so the cavity can be well-approximated by a qubit. In this scheme, both agent and environment qubits interact only with the register. In addition, concerning dissipative and depolarizing noise

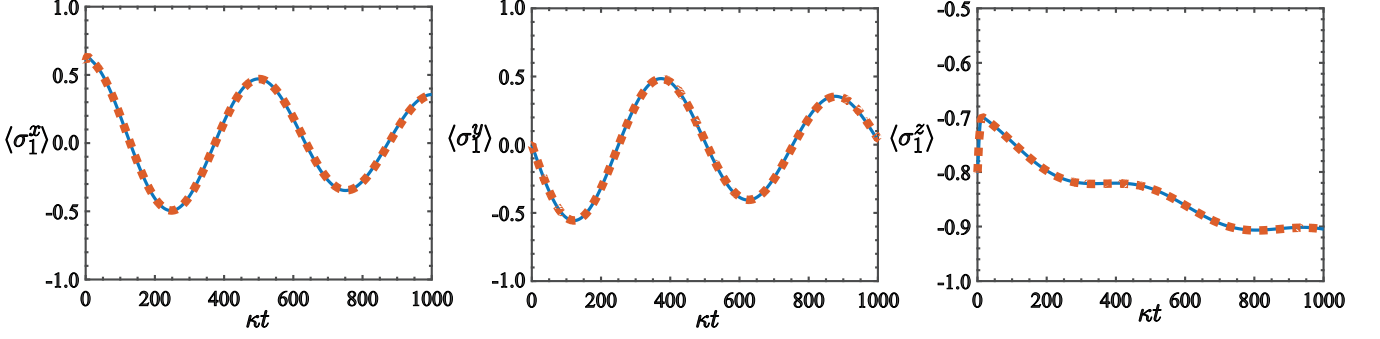


FIG. 2: Time evolution of the mean value of the qubit agent observables. Continuous blue line stand for the mean value computes through of analog dynamic and red dotted line corresponds to the mean value obtained as a machine learning protocol. The system parameters in this case are $\Delta_1 = \Delta_2 = J = 10\kappa$, $\delta_1 = \delta_2 = 0$, $g = 0.5\kappa$ and $\Omega = 5 \times 10^{-4}\kappa$. The initial state of the system is $|\Psi(0)\rangle = (\sqrt{0.9}|g\rangle + \sqrt{0.1}|e\rangle) \otimes (\sqrt{0.7}|g\rangle + \sqrt{0.3}|e\rangle) \otimes |0\rangle|0\rangle$, where $|e\rangle(|g\rangle)$ stands for the excited(ground) state of the qubits and $|0\rangle$ is the vacuum state of the cavity. In the digitized master equation, the time stets was taken by dividing the time step κt into 100 pieces.

channels, we consider two cases: (i) only the register is affected by noise, and (ii) all the qubits are affected by noise. The system dynamics can be described in general by the master equation

$$\dot{\rho}(t) = -i[\mathcal{H}, \rho] + \sum_k \sum_{\ell=1}^2 (2\mathcal{O}_{\ell k} \rho \mathcal{O}_{\ell k}^\dagger - \mathcal{O}_{\ell k}^\dagger \mathcal{O}_{\ell k} \rho - \rho \mathcal{O}_{\ell k}^\dagger \mathcal{O}_{\ell k}), \quad (6)$$

where $\mathcal{O}_{\ell k}$ are the collapse operators for each qubit given by $\mathcal{O}_{1k} = \sqrt{\gamma}\sigma_k^-$ for relaxation, and $\mathcal{O}_{2k} = \sqrt{\gamma_\phi}\sigma_k^z$ for depolarizing noise, and $k = A, R, E$ stands for agent, register and environment qubits, respectively, while \mathcal{H} is the system Hamiltonian written in the rotating frame with respect to the

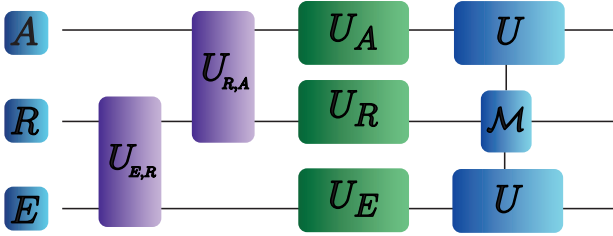


FIG. 3: Quantum circuit of a learning protocol with feedback, where A , E and R stand for agent, environment and register, respectively. The operations $U_{E,R}$, $U_{R,A}$ are acting in the environment-register and register-agent subspaces, respectively, and U_ℓ ($\ell = A, E, R$) represents a local conditional operation acting on each learning unit. \mathcal{M} stands for projective measurement on the register, the register is prepared in a given state depending of the measurement outcome and local conditional operations are applied on agent and environment subspaces.

driving field

$$\begin{aligned} \mathcal{H} = & \Pi(t_1)J(\sigma_R^+\sigma_E^- + \sigma_R^-\sigma_E^+) \\ & + \Pi(t_2)J(\sigma_R^+\sigma_A^- + \sigma_R^-\sigma_A^+) \\ & + \Pi(t_3)\left(\frac{\delta_A}{2}\sigma_A^z + \frac{\delta_E}{2}\sigma_E^z + \frac{\delta_R}{2}\sigma_R^z + \Omega\sigma_A^x\right). \quad (7) \end{aligned}$$

Here, σ_ℓ^k is the k -component Pauli matrix for the ℓ th two-level system, σ_ℓ^\pm stands for the ladder operator for the ℓ th qubit, $\delta_\ell = \omega_{q,\ell} - \omega_d$ is the detuning between the ℓ th qubit with respect to the driving field ω_d , and J is the exchange coupling strength. Additionally, t_i is the time step in which the Hamiltonian acts in the system dynamics and $\Pi(t)$ is the rectangle function defined as

$$\Pi(t_i) = \begin{cases} 0 & \text{if } |t_i| > \frac{1}{2} \\ \frac{1}{2} & \text{if } |t_i| = \frac{1}{2} \\ 1 & \text{if } |t_i| < \frac{1}{2} \end{cases} \quad (8)$$

The quantum machine learning protocol for this situation is depicted in Fig 3. The first stage in our protocol is to perform the Action i.e. we transfer information from the environment qubit and encode it in the register. To transfer the information we apply an analog block in the environment-register subspace represented by

$$U_{E,R} = e^{iJ(\sigma_R^+\sigma_E^- + \sigma_R^-\sigma_E^+)\Delta t}. \quad (9)$$

Afterwards, we perform the Percept which corresponds to transferring the register information towards the agent. Similar to the Action case, the transfer of information is done by applying a similar analog operation in the register-agent subspace,

$$U_{R,A} = e^{iJ(\sigma_R^+\sigma_A^- + \sigma_R^-\sigma_A^+)\Delta t}. \quad (10)$$

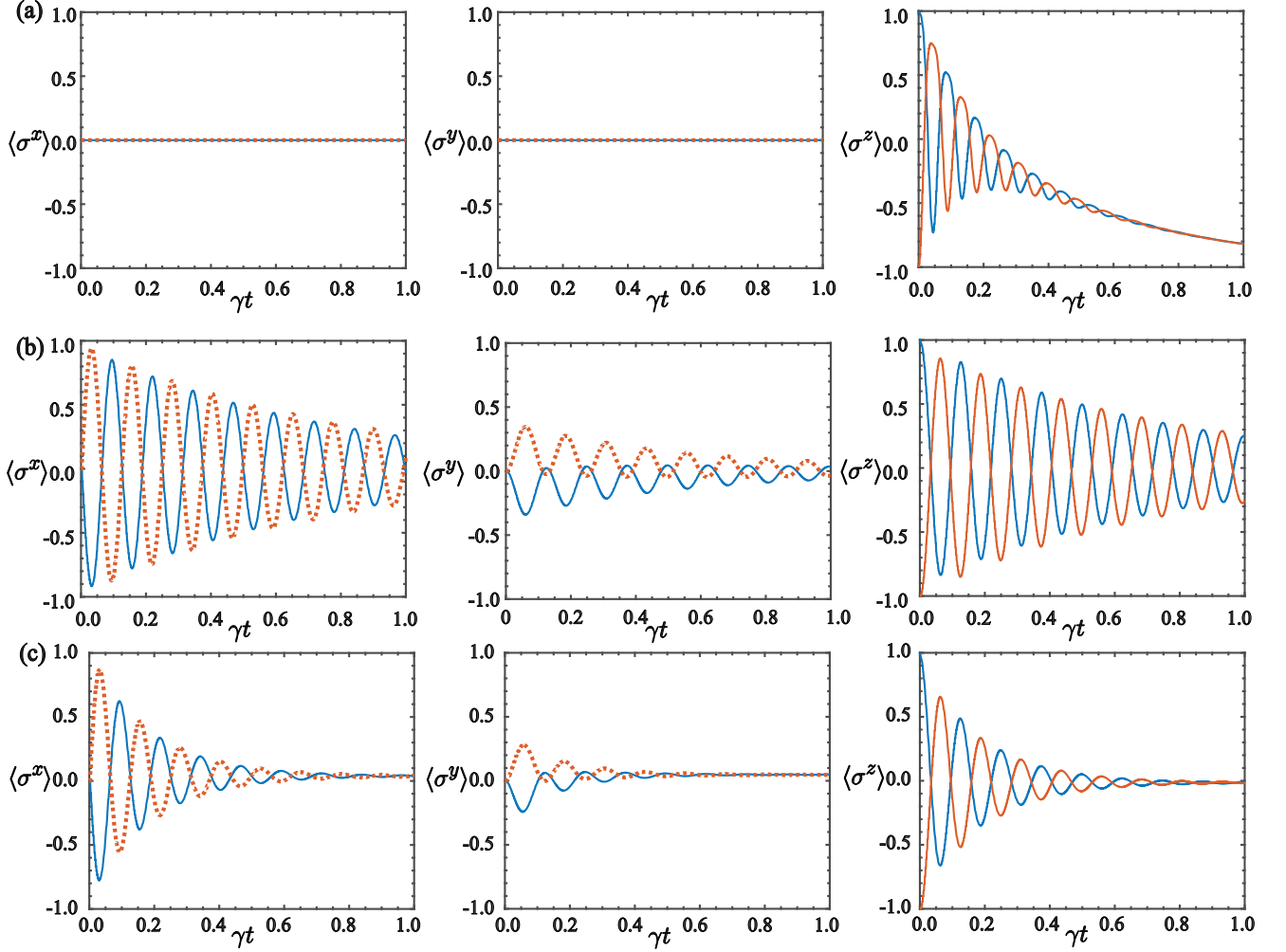


FIG. 4: Time evolution of the mean value of the qubits observables. The continuous blue line represents the mean value of Pauli matrices for the agent qubit, while red dotted line show the mean value of the environment qubit observables. (a) These plots represent the digital-analog process without feedback, (b) and (c) stand for the machine learning protocol with feedback for the aforementioned cases (i) and (ii). The system parameters are $\gamma = 2\gamma_\phi$, $\delta_A = \delta_R = \delta_E = 10\gamma$, $J = 50\gamma$ and $\Omega = 5 \times 10^{-4}\gamma$, and the initial state of the system is $|\Psi(0)\rangle = |e\rangle \otimes |g\rangle \otimes |g\rangle$.

Local operations on each subsystem are applied depending on the case under study (i) or (ii). The digital steps will correspond to the following operations.

Case (i): for the agent and the environment, the digital steps correspond to the dynamics of their respective free Hamiltonian represented by

$$U_A = e^{-i(\delta_A \sigma_A^z / 2 + \Omega \sigma_A^x) \Delta t}, \quad (11a)$$

$$U_E = e^{-i(\delta_E \sigma_E^z \Delta t / 2)}, \quad (11b)$$

while, for the register the digital step is the evolution given by

the master equation

$$\begin{aligned} \dot{\rho}(t) = & -i \left[\frac{\delta_R}{2} \sigma_R^z, \rho \right] \\ & + \sum_{\ell=1}^2 (2\mathcal{O}_{\ell R} \rho \mathcal{O}_{\ell R}^\dagger - \mathcal{O}_{\ell R}^\dagger \mathcal{O}_{\ell R} \rho - \rho \mathcal{O}_{\ell R}^\dagger \mathcal{O}_{\ell R}). \end{aligned} \quad (12)$$

Case (ii): for all the learning units (agent, register and environment) the digital step acting in them is given by the master equation

$$\begin{aligned} \dot{\rho}(t) = & -i \left[\frac{\delta_A}{2} \sigma_A^z + \frac{\delta_E}{2} \sigma_E^z + \frac{\delta_R}{2} \sigma_R^z + \Omega \sigma_A^x, \rho \right] \\ & + \sum_k \sum_{\ell=1}^2 (2\mathcal{O}_{\ell k} \rho \mathcal{O}_{\ell k}^\dagger - \mathcal{O}_{\ell k}^\dagger \mathcal{O}_{\ell k} \rho - \rho \mathcal{O}_{\ell k}^\dagger \mathcal{O}_{\ell k}), \end{aligned} \quad (13)$$

The next stage is to perform the feedback process involving measurement, reinitialization of the register state, and conditional local operations on the agent and environment subspace. The first step in the feedback process is to project the register in an eigenstate of σ^x . Depending on the measurement outcome, there are two conditional operations: if the register is projected in the state $|+\rangle$, we initialize the register in the state $|-\rangle$. Otherwise, if the register state is projected in $|-\rangle$, we initialize the register in $|+\rangle$ and we apply a local rotation in the agent and the register subspaces, represented by $U = e^{-i\pi\sigma_\ell^z/2}$, where $\ell = \{A, E\}$.

To elucidate how the quantum machine learning process with feedback mechanism enhances the synchronization, let us consider initial orthogonal states between agent and environment. Based on the figure of merit proposed in Ref [36] (the maximal fidelity between the agent state with the environment state is an indicator of a successful learning process), this is the worse situation for the learning process. Without loss of generality, the initial state of the system is $|\psi_0\rangle = |e\rangle_A \otimes |g\rangle_E \otimes |g\rangle_R$. Let us calculate the evolution for the expectation values of Pauli matrices for the agent and environment qubit, respectively, by iteratively applying the quantum machine learning protocol depicted in Fig 3. We will compare the result obtained for the aforementioned cases (i) and (ii) with the case without feedback mechanism. These results are depicted in Fig 4. In the machine learning protocol without feedback in Fig 4(a) the average of $\langle\sigma^x\rangle$ and $\langle\sigma^y\rangle$ do not exhibit any oscillation, since due to the interaction in Hamiltonian given by Eq. (7) and the initial state $|\psi_0\rangle$, the system only evolves in the subspace composed of states with one excitation i.e. $\{|e, g, g\rangle, |g, e, g\rangle, |g, g, e\rangle\}$. Thus, the expectation value for operators σ_ℓ^x and σ_ℓ^y always vanishes. On the contrary, σ_ℓ^z acting on the state introduces a local phase on the state depending if the state is in $|e\rangle$ or $|g\rangle$, then $\langle\sigma_\ell^z\rangle \neq 0$ as depicted in Fig 4(a). As we can see in Fig 4(b) and Fig 4(c), including feedback process, the initialization of the register state in an eigenstate of σ^x yields the system to evolve in a subspace of one and two excitation states, hence, $\langle\sigma_\ell^x\rangle$, $\langle\sigma_\ell^y\rangle$ and $\langle\sigma_\ell^z\rangle$ are different from zero. As a result, the synchronization is improved when compared with the case without feedback mechanism. Fig 5(b) (case (i)) differs from Fig 5(c) (case (ii)) mainly in that the presence of noisy channels acting in all the learning units produces a harmful effect on the evolution of the expectation values, i.e. the expectation values decrease faster than in case (i). However, despite this additional detrimental effect, the feedback mechanism still provides an enhancement in the synchronization.

Since the feedback mechanism described here produces a change in the subspace of the system evolution, this effect can be interpreted as an effective environment engineering process, in the sense that, the dark state at which the system must converge is changed because of the measurement and the local conditional operations. Thus, by changing the feedback mechanism (learning strategy), we could be capable of modifying the state in which the agent and the environment synchronizes.

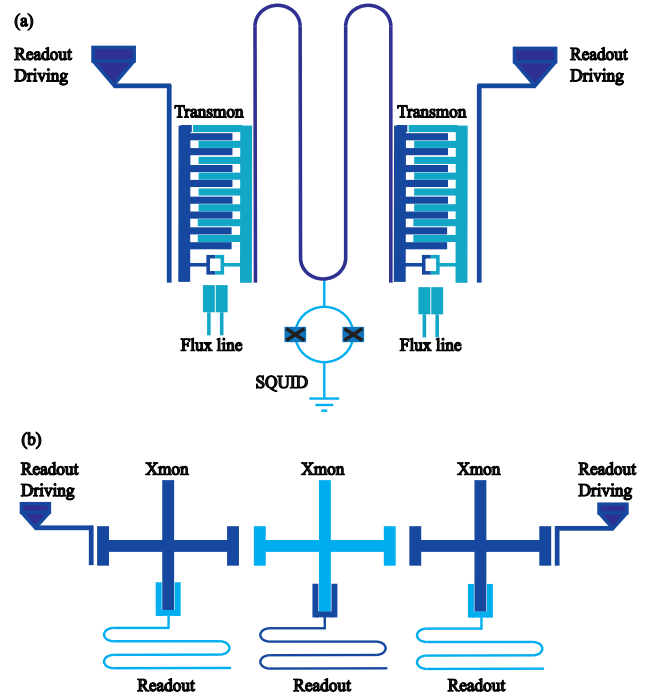


FIG. 5: Scheme of the experimental proposal. (a) Two superconducting $\lambda/4$ coplanar waveguide resonator are galvanically coupled to each other through a SQUID. In addition, at the edge of each resonator, a transmon device is capacitively coupled to the resonator. (b) Three superconducting Xmon qubits are coupled capacitively to each other.

IMPLEMENTATION IN SUPERCONDUCTING CIRCUITS

Our proposal can be implemented in a circuit quantum electrodynamic architecture with current technology. Indeed, for the realization of the qubit-cavity setup, current technology allows us to connect charge qubits and flux qubits to a microwave transmission line resonators. Our setup, depicted in Fig 5(a) is composed of two $\lambda/4$ transmission line resonator coupled by a superconducting interference device (SQUID) through the current. This coupling allows us to tune the cavity frequency and the coupling strength between each resonator [37–40]. Moreover, two transmon qubits [41] are capacitively coupled to the resonator through the voltage at the ends of the transmission line resonator. We choose charge qubits instead of flux qubit because charge qubits have coherence times larger than the flux qubits [42–45]. For the machine learning protocol implemented with qubits, our proposal based on circuit quantum electrodynamics architecture can be implemented by considering arrays of Xmon qubits [46–48], as shown in Fig 5(b). Xmon qubits offer high coherence times and fast tunability.

Current technology has made possible the implementation of quantum feedback in superconducting circuits [49–51]. A system based on a closed-loop circuit together with binary measurement has allowed to implement a protocol to rapidly reinitialize the state of a qubit, this process is done in a time

scale at least one order of magnitude faster than the relaxation time of the two-level system [49, 50]. In addition, current technologies based on transmon qubits coupled to a microwave resonator has made possible to implement weak measurements, this weak measurement mechanism has allowed to monitor the Rabi oscillation between qubit states as well as to reconstruct a quantum state [51].

CONCLUSION

We have shown that quantum synchronization between a pair of two-level system is achieved by considering the digital-analog decomposition of the master equation which governs the system dynamics. We can identify in this block decomposition the fundamental elements of a quantum machine learning protocol, namely, agent, environment and register. Afterwards, we have also equipped the machine learning protocol with a feedback mechanism based on measurements and reinitialization of the register state together with conditional local operations on the agent and environment subspace, substantially increasing its power and flexibility. Indeed, numerical simulations show an enhancement in the synchronization manifested in the number of operators that synchronizes and the rate in which the synchronization is achieved. Furthermore, by modifying the protocol, we may choose the state in which the system synchronizes. Finally, based on current technologies on superconducting circuit and quantum electrodynamics, we have proposed and implementation of the quantum machine learning protocol with feedback.

ACKNOWLEDGMENTS

We would like to thank L. Lamata and Daniel Z. Rossatto for the useful discussions. F.A.C.-L. acknowledges support from CEDENNA basal grant No. FB0807 and Dirección de Postgrado USACH. J. C. R. acknowledges the support from FONDECYT under grant No. 1140194. M. S. and E. S. acknowledge support from Spanish MINECO/FEDER FIS2015-69983-P and Basque Government IT986-16.

* Corresponding authors:

francisco.cardenas@usach.cl

† mikel.sanz@ehu.es

- [1] R. S. Michalski, J. G. Carbonell, and T. M. Mitchell *Machine learning: An artificial intelligence approach* (Springer Science & Business Media, 2013)
- [2] E. Boros, P. L. Hammer, T. Ibakari, A. Kogan, E. Mayoraz, and I. Muchnik. An implementation of logical analysis of data. *IEEE Transactions on Knowledge and Data Engineering* **12**, 292 (2000).
- [3] N. Lavra, Selected techniques for data mining in medicine. *Artificial intelligence in Medicine* **16**, 3 (1999).
- [4] I. Kononenko, Machine learning for medical diagnosis: history, state of the art and perspective. *Artificial Intelligence in Medicine* **23**, 89 (2001).
- [5] K.-F. Lee, H.-W. Hon, M.-Y. Hwang, S. Mahajan, and R. Reddy, The SPHINX speech recognition system. *Acoustics, Speech, and Signal Processing* (1989).
- [6] R. Palmoodon and S. N. Srihari, Online and off-line handwriting recognition: a comprehensive survey. *IEEE Transactions on Pattern Analysis and Machine Intelligence* **22**, 63 (2000).
- [7] G. Bello-Orgaz, J.J. Jung, and D. Camacho, Social big data: Recent achievements and new challenges. *Information Fusion* **28**, 45 (2016).
- [8] S. J. Russell and P. Norvig, *Artificial Intelligence: A Modern Approach (International Edition)* (Pearson US Imports & PHIPEs, 2002).
- [9] R. S. Sutton and A. G. Barto, *Reinforcement learning: An introduction, Vol. 1* (MIT press Cambridge, 1998).
- [10] L. Lamata, U. Alvarez-Rodriguez, J. D. Martín-Guerrero, M. Sanz, E. Solano, arXiv:1709.07409 (2017).
- [11] N. Spagnolo, E. Maiorino, C. Vitelli, M. Bentivegna, A. Crespi, R. Ramponi, P. Mataloni, R. Osellame, and F. Sciarrino, arXiv:1610.03291 (2016).
- [12] A. Pikovsky, M. Rosenblum, and J. Kurths, *Synchronization: a universal concept in nonlinear sciences, Vol. 12* (Cambridge University Press, UK, 2003).
- [13] A. C. Luo, *Dynamical system synchronization* (Springer, 2013).
- [14] M. Steriade, Synchronized activities of coupled oscillators in the cerebral cortex and thalamus at different levels of vigilance. *Cerebral Cortex* **7**, 583 (1997).
- [15] S. Yamaguchi, H. Isejima, T. Matsuo, R. Okura, K. Yagita, M. Kobayashi, and H. Okamura, Synchronization of Cellular Clocks in the Suprachiasmatic Nucleus. *Science* **302**, 1408 (2003).
- [16] M. Rohden, A. Sorge, M. Timme, and D. Witthaut, Self-Organized Synchronization in Decentralized Power Grids. *Phys. Rev.Lett.* **109**, 064101 (2012).
- [17] D. Leibfried, R. Blatt, C. Monroe, and D. Wineland, Quantum dynamics of single trapped ions. *Rev. Mod. Phys.* **75**, 281 (2003).
- [18] H. Häffner, C. Roos, and R. Blatt, Quantum computing with trapped ions. *Physics Reports* **469**, 155 (2008).
- [19] M. D. LaHaye, O. Buu, B. Camarota, and K. C. Schwab, Approaching the Quantum Limit of a Nanomechanical Resonator. *Science* **304**, 74 (2004).
- [20] J. Chan, T. P. M. Alegre, A. H. Safavi-Naeini, J. T. Hill, A. Krause, S. Gröblacher, M. Aspelmeyer, and O. Painter, Laser cooling of a nanomechanical oscillator into its quantum ground state. *Nature* **478**, 89 (2011).
- [21] M. Aspelmeyer, T. J. Kippenberg, and F. Marquardt, Cavity optomechanics. *Rev. Mod. Phys.* **86**, 1391 (2014).
- [22] A. Blais, J. Gambetta, A. Wallraff, D. I. Schuster, S. M. Girvin, M. H. Devoret, and R. J. Schoelkopf, Quantum-information processing with circuit quantum electrodynamics. *Phys. Rev. A* **75**, 032329 (2007).
- [23] J. Clarke and F. K. Wilhelm, Superconducting quantum bits. *Nature* **453**, 1031 (2008).
- [24] G. Wendin, Quantum information processing with superconducting circuits: a review. *Rep. Prog. Phys.* **80**, 106001 (2017).
- [25] T. E. Lee and H. R. Sadeghpour, Quantum Synchronization of Quantum van der Pol Oscillators with Trapped Ions. *Phys. Rev. Lett.* **111**, 234101 (2013).
- [26] G. Manzano, F. Galve, G. L. Giorgi, E. Hernández-García, and R. Zambrini, Synchronization, quantum correlations and entanglement in oscillator networks. *Sci. Rep.* **3**, 1439 (2013).

- [27] M. R. Hush, W. Li, S. Genway, I. Lesanovsky, and A. D. Armour, Spin correlations as a probe of quantum synchronization in trapped-ion phonon lasers. *Phys. Rev. A* **91**, 061401 (2015).
- [28] S. Walter, A. Nunnenkamp, and C. Bruder, Quantum Synchronization of a Driven Self-Sustained Oscillator. *Phys. Rev. Lett.* **112**, 094102 (2014).
- [29] K. Wiesenfeld, P. Colet, and S. H. Strogatz, Synchronization Transitions in a Disordered Josephson Series Array. *Phys. Rev. Lett.* **76**, 404 (1996).
- [30] T. E. Lee, C.-K. Chan, and S. Wang, Entanglement tongue and quantum synchronization of disordered oscillators. *Phys. Rev. E* **89**, 022913 (2014).
- [31] M. H. Matheny, M. Grau, L. G. Villanueva, R. B. Karabalin, M. C. Cross, and M. L. Roukes, Phase Synchronization of Two Anharmonic Nanomechanical Oscillators. *Phys. Rev. Lett.* **112**, 014101 (2014).
- [32] O. V. Zhirov and D. L. Shepelyansky, Synchronization and Bistability of a Qubit Coupled to a Driven Dissipative Oscillator. *Phys. Rev. Lett.* **100**, 014101 (2008).
- [33] O. V. Zhirov and D. L. Shepelyansky, Quantum synchronization and entanglement of two qubits coupled to a driven dissipative resonator. *Phys. Rev. B* **80**, 014519 (2009).
- [34] G. L. Giorgi, F. Plastina, G. Francica, and R. Zambrini, Spontaneous synchronization and quantum correlation dynamics of open spin systems. *Phys. Rev. A* **88**, 042115 (2013).
- [35] H. Eneriz, D. Rossatto, M. Sanz, and E. Solano, Degree of Quantumness in Quantum Synchronization. arXiv:1705.04614 (2017).
- [36] L. Lamata, Basic protocols in quantum reinforcement learning with superconducting circuits. *Sci. Rep.* **7**, 1609 (2017).
- [37] S. Felicetti, M. Sanz, L. Lamata, G. Romero, G. Johansson, P. Delsing, and E. Solano, Dynamical Casimir Effect Entangles Artificial Atoms. *Phys. Rev. Lett.* **113**, 093602 (2014).
- [38] D. Z. Rossatto, S. Felicetti, H. Eneriz, E. Rico, M. Sanz, and E. Solano, Entangling polaritons via dynamical Casimir effect in circuit quantum electrodynamics. *Phys. Rev. B* **93**, 094514 (2016).
- [39] F. Wulschner, J. Goetz, F. R. Koessel, E. Hoffmann, A. Baust, P. Eder, M. Fischer, M. Haerberlein, M. J. Schwarz, M. Pernpeintner, E. Xie, L. Zhong, C. W. Zollitsch, B. Peropadre, J.-J. Garcia Ripoll, E. Solano, K. G. Fedorov, E. P. Menzel, F. Deppe, A. Marx, and R. Gross, Tunable coupling of transmission-line microwave resonators mediated by an rf SQUID. *EPJ Quantum Technology* **3**, 10 (2016).
- [40] Y. Nakashima, F. Hirayama, S. Kohjiro, H. Yamamori, S. Nagasawa, N. Y. Yamasaki, and K. Mitsuda, Adjustable SQUID-resonator direct coupling in microwave SQUID multiplexer for TES microcalorimeter array. *IEICE Electronics Express* **14**, 20170271 (2017).
- [41] J. Koch, T. M. Yu, J. Gambetta, A. A. Houck, D. I. Schuster, J. Majer, A. Blais, M. H. Devoret, S. M. Girvin, and R. J. Schoelkopf, Charge-insensitive qubit design derived from the Cooper pair box. *Phys. Rev. A* **76**, 042319 (2007).
- [42] C. Rigetti, J. M. Gambetta, S. Poletto, B. L. T. Plourde, J. M. Chow, A. D. Córcoles, J. A. Smolin, S. T. Merkel, J. R. Rozen, G. A. Keefe, M. B. Rothwell, M. B. Ketchen, and M. Steffen, Superconducting qubit in a waveguide cavity with a coherence time approaching 0.1 ms. *Phys. Rev. B* **86**, 100506 (2012).
- [43] K. L. Geerlings, *Improving coherence of superconducting qubits and resonators* (PhD Thesis, Yale University, 2013).
- [44] E. Lucero, M. Steffen, J. Gambetta, D. Abraham, A. Corcoles, and Q. C. Team, *APS Meeting Abstracts* (2013).
- [45] R. Barends, et al., Digitized adiabatic quantum computing with a superconducting circuit. *Nature* **534**, 222 (2016).
- [46] R. Barends, J. Kelly, A. Megrant, D. Sank, E. Jeffrey, Y. Chen, Y. Yin, B. Chiaro, J. Mutus, C. Neill, P. O'Malley, P. Roushan, J. Wenner, T. C. White, A. N. Cleland, and J. M. Martinis, Coherent Josephson Qubit Suitable for Scalable Quantum Integrated Circuits. *Phys. Rev. Lett.* **111**, 080502 (2013).
- [47] M. R. Geller, E. Donate, Y. Chen, M. T. Fang, N. Leung, C. Neill, P. Roushan, and J. M. Martinis, Tunable coupler for superconducting Xmon qubits: Perturbative nonlinear model. *Phys. Rev. A* **92**, 012320 (2015).
- [48] Y. Chen, C. Neill, P. Roushan, N. Leung, M. Fang, R. Barends, J. Kelly, B. Campbell, Z. Chen, B. Chiaro, A. Dunsworth, E. Jeffrey, A. Megrant, J. Y. Mutus, P. J. J. O'Malley, C. M. Quintana, D. Sank, A. Vainsencher, J. Wenner, T. C. White, M. R. Geller, A. N. Cleland, and J. M. Martinis, Qubit Architecture with High Coherence and Fast Tunable Coupling. *Phys. Rev. Lett.* **113**, 220502 (2014).
- [49] D. Ristè, C. C. Bultink, K. W. Lehnert, and L. DiCarlo, Feedback Control of a Solid-State Qubit Using High-Fidelity Projective Measurement. *Phys. Rev. Lett.* **109**, 240502 (2012).
- [50] D. Ristè and L. DiCarlo, arXiv:1508.01385 (2015).
- [51] K. W. Murch, R. Vijay, and I. Siddiqi, *Superconducting Devices in Quantum Optics*, edited by R. H. Hadfield and G. Johansson (Springer International Publishing, Cham, 2016)